

Micromotion compensation in a surface electrode ion trap

Kenneth R. Brown, Robert J. Clark, Jaroslaw Labaziewicz, Philip Richerme, David R. Leibrandt, and Isaac L. Chuang
*Center for Bits and Atoms, Research Laboratory of Electronics, & Department of Physics
Massachusetts Institute of Technology, Cambridge, Massachusetts 02139, USA*
(Dated: February 9, 2020)

The promise of a surface electrode geometry for realizing complex multi-zone ion traps is challenged by the difficulty of compensating trap potentials to remove undesired micromotion, caused by stray surface charges and intrinsic electrode asymmetry. We demonstrate a micromotion compensation procedure using trapped strontium ions in a ~ 1 mm-scale five-electrode trap, which works despite trap depths of ~ 0.5 eV, using buffer gas cooling, resulting in a micromotion amplitude of less than $0.2 \mu\text{m}$.

Surface electrode ion traps [1–3] offer significant potential for realizing complicated geometries needed for large-scale quantum computation [4]. Their advantages include greater ease of fabrication than three dimensional (3D) layered planar traps [5, 6] and the ability to integrate control electronics below the electrode surface [7]. Two major challenges which must be overcome, however, are the shallow trap depth intrinsic to a 2D geometry, which is $\sim 1/100$ of comparably sized 3D traps [1], and the need for unusual compensation voltages to reduce ion heating to the minimum levels needed for quantum control of ion motion. A variety of approaches can deal with the shallow depth problem [2, 3]. Finding compensation voltages requires both an initial calculation to account for the trap geometry and then experimentally determining the precise voltages [3].

The art of compensation, well developed for traditional 3D ion traps [8–10], is essential in removing systematic and stray electric fields which prevent an ion from sitting at the zero point of the trap radiofrequency (rf) field. Without dc compensation voltages carefully applied, usually to special electrodes placed around the ion, static fields created by stray charges on dielectrics typically cause undesired heating of ions; this results from coupling of the rf driven “micromotion” of one ion with the secular motion of neighboring ions. Fortunately, the natural symmetry of traditional 3D Paul traps simplifies compensation voltage needs, and limits dielectric where stray charges can build up.

However, surface electrode Paul traps inherently require special attention to compensation voltage needs. First, due to the radial asymmetry of the trap, the axial trapping potential results in an undesired static electric field which must be compensated for. In Ref. [3] extra electrodes were designed specifically to cancel this field. Second, the trap substrate, typically an insulating dielectric, is susceptible to charge buildup resulting in stray fields which also must be compensated for. Finally, experimentally determining the proper compensation voltages when using electron bombardment ionization is difficult due to the shallow trap depth and relatively large stray fields caused by charge buildup.

Here, we demonstrate one method to address micro-

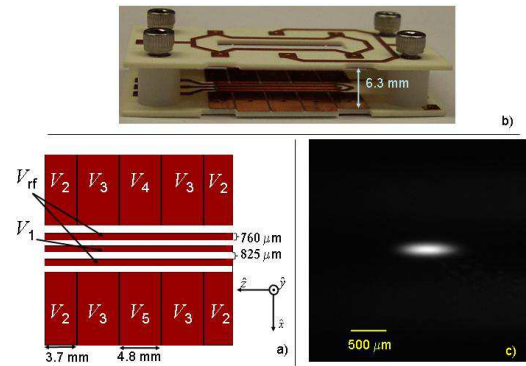


FIG. 1: (a) Layout of trap electrodes, each labeled with the voltage applied; all but V_{rf} are dc. The space around the long electrodes (V_{rf} and V_1) has been milled out. Coordinates referenced as shown define the origin at the trap center and on the chip surface. (b) Photograph showing the top electrode plate mounted 6.3 mm above the trap. The top plate has a slit for ion fluorescence detection; a dc voltage V_{top} applied to it can deepen the trap depth. (c) CCD image showing strontium ions trapped in the middle of the trap.

motion compensation, by determining the compensation voltages in the presence of a non-reactive gas that enhances trap stability through collisional damping of hot ion motion. This buffer gas [11, 12] stabilizes the trap sufficiently to allow measurement and minimization of the undesired micromotion. After the compensation correction procedure, ions can be loaded at ultra-high vacuum (UHV) and stored with long lifetimes.

We demonstrate this compensation method using strontium ions in a ~ 1 mm-scale surface electrode trap. Following the design of a traditional four-rod linear Paul trap system [13], the trap is mounted in a standard UHV chamber pumped down to $\sim 10^{-9}$ torr, loaded with $^{88}\text{Sr}^+$ by electron bombardment ionization of neutral atoms from a resistive oven source, and driven by a helical resonator mounted externally. An optional, controlled buffer gas environment of up to 10^{-4} torr of ultra-pure helium is provided through a sensitive leak valve, monitored with a Bayard-Alpert ion gauge.

Our surface electrode ion trap has five electrodes [1, 2]:

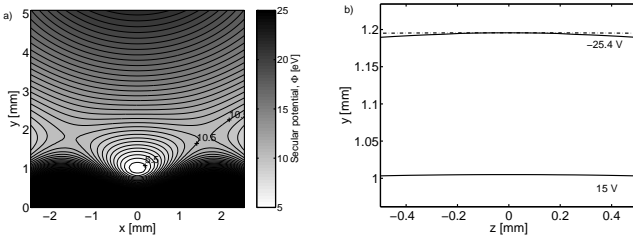


FIG. 2: (a) Cross-section of the pseudopotential along the \hat{x} and \hat{y} directions, for $V_{rf} = 1260$ V at $\Omega/2\pi = 7.6$ MHz, with $V_{top} = 15$ V, $V_2 = 110$ V, and $V_3 = -50$ V. (b) Calculated rf node (dashed line) and ion cloud locations (solid lines) for $V_{top} = 15$ and -25.4 V.

one center electrode at ground, two at rf potential, and two segmented dc electrodes (Fig. 1). The electrodes are copper, deposited on a low rf loss substrate, Rogers 4350B, and fabricated by Hughes circuits following standard methods for microwave circuits. In the loading region, slots are milled between the rf and dc electrodes to prevent shorting due to strontium buildup. The inner surfaces are plated with copper to minimize trap potential distortion due to accumulation of stray surface charges. The trap surface is polished to a $1\ \mu\text{m}$ finish to reduce laser scatter into the detector.

Ions are detected by laser induced fluorescence of the main $422\ \text{nm}$ $5S_{1/2} \rightarrow 5P_{1/2}$ transition of strontium [13], using either an electron-multiplying CCD camera (Princeton Instruments PhotonMax) or a photomultiplier tube (Hamamatsu H6780-04). A laser tuned to $1092\ \text{nm}$ addresses the $5P_{1/2} \rightarrow 4D_{3/2}$ transition to prevent shelving from the P state to the metastable D state. The two external cavity laser diode sources are optically locked to low finesse cavities [14]. Typical laser powers at the trap center are $1.2\ \text{mW}$ at $1092\ \text{nm}$ and $20 - 50\ \mu\text{W}$ at $422\ \text{nm}$.

The first step in micromotion compensation of a surface electrode trap is determination of the ideal compensation voltages needed to offset the inherent asymmetry. We determine these potentials numerically (using CPO, a boundary element electrostatic solver [15]), by computing the rf and dc potentials ($\phi_{rf} \cos \Omega t$ and ϕ_{dc}), which give the secular potential $\Phi = Q^2 |\nabla \phi_{rf}|^2 / 4m\Omega^2 + Q\phi_{dc}$ where m is the ion mass and Q is the ion charge. Typically, V_{rf} is of 500 - 1200 V amplitude at $\Omega/2\pi = 7.6$ MHz, and dc electrode voltages (as defined in Fig. 1) are $V_4 = V_5 = 0$ V, $V_2 = 110$ V, and $V_3 = -50$ V. Shown in Fig. 2 is a cross-section of the secular potential in the \hat{x} - \hat{y} plane, at $z = 0$. As indicated in the figure, with these voltages, and $V_{top} = -25.4$ V applied to the top electrode, the trap should be compensated with a trap depth of $0.5\ \text{eV}$. The trap depth can be increased to $5.4\ \text{eV}$ by setting $V_{top} = 15$ V, at the cost of increased micromotion.

These ideal compensation voltages often differ substan-

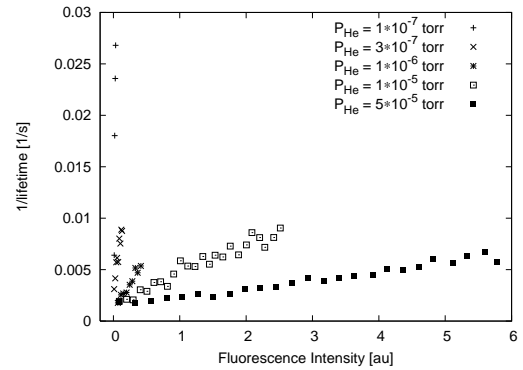


FIG. 3: Plot of $1/\text{lifetime}$ as a function of fluorescence intensity at five different buffer gas pressures in an uncompensated trap. These data show that long lifetimes can be obtained at nearly any buffer gas pressure but at very different cloud sizes as measured by fluorescence intensity. The optimum settings, long lifetimes and large clouds, are obtained at high buffer gas pressure.

tially from actual ones, due to the presence of unknown stray charges in the trap. A variety of techniques have been developed to experimentally determine the appropriate voltages, including examination of the single ion spectrum [9, 10], the correlation between ion fluorescence and the rf drive phase [8], and the change in ion position with pseudopotential depth [8]. The first two methods require cold and small ion clouds necessitating good initial compensation. The last method is more widely applicable, but requires observable clouds of ions to be loaded with reasonably long lifetime.

We employ buffer gas cooling to load and maintain the large ion clouds needed for experimental determination of appropriate compensation voltages. Initially, when the cloud center is $0.2\ \text{mm}$ from the rf node, the size and lifetime of the loaded cloud depends strongly on the buffer gas pressure (Fig. 3). Notably, lifetimes at UHV were too short to be measured in the uncompensated trap. Based on the data in Fig. 3, we perform our compensation experiments at 1×10^{-5} torr. This pressure yields an excellent signal to noise ratio (~ 200 for a $50\ \text{ms}$ integration time with the PMT) and long ion lifetime ($\sim 300\ \text{s}$) without overburdening the ion pump. The ion temperature was determined to be $2000\ \text{K}$ by the Doppler profile.

An accurate value of the stray dc field can be calculated from the cloud motion using the following model. The electric field along a coordinate x , at the rf node, is well approximated by $E(x) = E_0 + E_1 x$. For an rf pseudopotential with secular frequency ω , the ion motion follows $m\ddot{x} + m\omega^2 x + eE(x) = 0$, which results in a new secular frequency $\omega_1 = \sqrt{\omega^2 + eE_1/m}$, and a new cloud center position $x_0 = eE_0/m\omega_1^2$. By measuring both the secular frequency and the ion center, one can determine E_0 .

We experimentally determine E_0 by measuring the

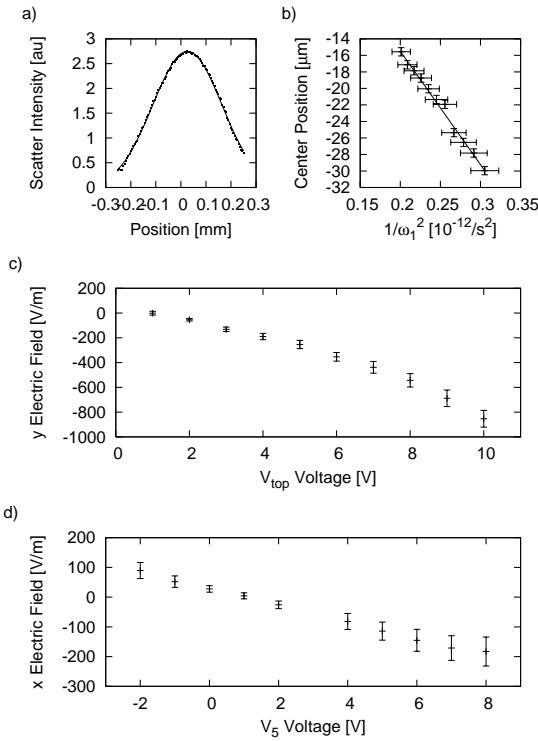


FIG. 4: Measurement results showing compensation of micro-motion in the trap at a buffer gas pressure of 1×10^{-5} torr. (a) Cloud intensity profile along the \hat{y} axis, fit to a Gaussian, for a representative value of the the \hat{y} compensation voltage, V_{top} . (b) Linear fit of the cloud center position versus $1/\omega_1^2$ where ω_1 is the secular frequency of the ion motion, yielding the electric field along \hat{y} at the rf node. (c) Plot of the \hat{y} electric field as a function of the V_{top} compensating voltage, showing that the stray field is minimized at $V_{top} = 1.0$ V. (d) Plot of the \hat{x} electric field as a function of the middle electrode voltage V_5 , showing compensation at $V_5 = 1.3$ V.

cloud center position as a function of applied voltages. The 1092 nm laser is configured to illuminate the entire trapping region, while the 422 nm laser is focused to a $60 \mu\text{m}$ spot; the focal point is translated in the \hat{x} - \hat{y} plane by using a precision motorized stage. Ion cloud fluorescence intensity, measured by the PMT, is recorded as a function of laser position, and fit to a Gaussian centered at the ion cloud position [16]. This measurement is then repeated at 10 different rf voltages, and a linear fit of the cloud center positions to $1/\omega_1^2$ determines the stray dc field value E_0 .

The data obtained, shown in Fig. 4, give an excellent match of the cloud intensity to a Gaussian fit, allowing measurement of the cloud center to within $\pm 0.5 \mu\text{m}$. Thus, the measurement of stray fields is precise to about $\pm 10\text{V/m}$ at zero stray field. From the stray field measurements, we determine the required compensation voltages to be $V_{top} = 1.0 \pm 0.1$ V and $V_5 = 1.3 \pm 0.3$ V. The estimated residual micromotion of a single ion at these voltages is less than $0.2 \mu\text{m}$. The nonlinear dependence

of the dc electric field along \hat{y} on the top electrode voltage is due to the strong anharmonicity of the trap in the vertical direction, unaccounted for in the simple linear model employed in the analysis.

The difference between measured and ideal compensation voltages is evidence of anisotropic stray fields, caused by undetermined surface charges. The estimated stray fields along \hat{x} are comparable to those reported for 3D traps [8]. However, the stray fields along \hat{y} are 10 times larger. The 26 V difference between the calculated and measured values of V_{top} at compensation suggests significant electron charging on either the trap surface, the top plate, or the top observation window.

We have shown that micromotion compensation in a surface electrode ion trap can be challenging due to the inherent design of the trap, but may be successfully accomplished using buffer gas cooling to allow initial loading of observable ion clouds. These results suggest that special efforts will be needed to prevent possible stray surface charges, perhaps by attention to electron gun collimation, or by photoionization loading [3]. The techniques demonstrated will likely be useful for practical investigation of a variety of complex and integrated surface electrode ion trap schemes, enabling resolution of micromotion heating issues with sequenced ion movement and crosstalk between multiple-zone ion trap electrodes.

Support for this project was provided in part by the JST/CREST Urabe Project, and MURI project F49620-03-1-0420. We thank Rainer Blatt, Richart Slusher, Vladan Vuletic, and David Wineland for helpful discussions.

- [1] J. Chiaverini, R. B. Blakestad, J. Britton, J. D. Jost, C. Langer, D. Leibfried, R. Ozeri, and D. J. Wineland, Quant. Inf. and Comp. **5**, 419 (2005).
- [2] C. E. Pearson, D. R. Leibrandt, W. S. Bakr, W. J. Maldard, K. R. Brown, and I. L. Chuang, Phys. Rev. A to appear (2006), quant-ph/0511018.
- [3] S. Seidelin, J. Chiaverini, R. Reichle, J. J. Bollinger, D. Leibfried, J. Britton, J. H. Wesenberg, R. B. Blakestad, R. J. Epstein, D. B. Hume, J. D. Jost, C. Langer, R. Ozeri, and D. J. Wineland, quant-ph/0601173.
- [4] D. Kielpinski, C. Monroe, and D. J. Wineland, Nature **417**, 709 (2002).
- [5] M. J. Madsen, W. K. Hensinger, D. Stick, J. A. Rabchuk, and C. Monroe, Appl. Phys. B **78**, 639 (2004).
- [6] D. Stick, W. K. Hensinger, S. Olmschenk, M. J. Madsen, K. Schwab, and C. Monroe, Nature Physics **2**, 36 (2006).
- [7] J. Kim, S. Pau, Z. Ma, H. R. McLellan, J. V. Gates, A. Kornblit, R. E. Slusher, R. M. Jopson, I. Kang, and M. Dinu, Quant. Inf. Comp. **5**, 515 (2005).
- [8] D. J. Berkeland, J. D. Miller, J. C. Bergquist, W. M. Itano, and D. J. Wineland, J. Appl. Phys. **83**, 5025 (1998).
- [9] C. Raab, J. Eschner, J. Bolle, H. Oberst, F. Schmidt-

Kaler, and R. Blatt, Phys. Rev. Lett. **85**, 538 (2000).

[10] C. Lisowski, M. Knoop, C. Champenois, G. Hagel, M. Vedel, and F. Vedel, Appl. Phys. B **81**, 5 (2005).

[11] H. G. Dehmelt, Adv. At. Mol. Phys. **5**, 109 (1969).

[12] Y. Moriwaki, M. Tachikawa, Y. Maeno, and T. Shimizu, Jpn. J. Appl. Phys. **31**, L1640 (1992).

[13] D. J. Berkeland, Rev. Sci. Inst **73**, 2856 (2002).

[14] K. Hayasaka, Opt. Comm. **206**, 401 (2002).

[15] B. Brkić, S. Taylor, J. F. Ralph, and N. France, Phys. Rev. A **73**, 012326 (2006).

[16] I. Siemers, R. Blatt, T. Sauter, and W. Neuhauser, Phys. Rev. A **38**, 5121 (1988).